InSAS'00: Interferometric SAS and INS aided SAS imaging

L. Wang, A. Bellettini, R. Hollett, A. Tesei, M. Pinto,
NATO SACLANT Undersea Research Centre, La Spezia, Italy,
S. Chapman, QinetiQ, Bincleaves, UK
K. Gade, FFI, Kjeller, Norway

***Abstract*- This paper presents results of an experiment carried out in Elba Island (Italy), aimed at investigating wideband interferometric synthetic aperture sonar (InSAS). A 20 m underwater rail with a multi-axis motion actuator (MAMA) was used to introduce controlled distortions in the sonar trajectory during its displacement along the rail. The sonar operated between 120 kHz and 180 kHz and consisted of two 32 channel receiver arrays, of length L=26.7 cm, vertically separated by 21 cm, and of three transmitters spaced along-track at L/2. A very high grade Inertial Navigation System (INS), of the 0.1 nm/hr class was used to sense the sonar motion. Raw sonar and INS data were collected under various pre-determined distortions, e.g. ±1° sinusoidal yaw, for offline analysis. Multi-aspect insonification of different objects were also carried out using a turntable in order to assess the benefit for object classification.**

High navigational accuracy is obtained by combining INS motion estimates with those derived from the DPCA (Displaced Phase Centre Antenna), making very high resolution SAS imagery possible. Images with along-track resolution gains of Q=50-100 compared to that of the physical array are obtained in the presence of ±1° sinusoidal yaw.

I. INTRODUCTION

Interferometric Synthetic Aperture Sonar (InSAS) can provide co-registered images and bathymetry, with much higher along-track resolution than conventional sonar, hence enables better detection and classification of underwater objects, man made or natural. Therefore it offers great potential in underwater operations.

In order to combine coherently the received echoes across the whole length of an SAS, the sonar trajectory has to be measured accurately, typically within a fraction of a wavelength. It is not realistic in general to assume that the sonar travels along a straight track at constant speed. In practice, the motion is perturbed randomly from this ideal trajectory due to the combination of variable driving forces, such as towing from a cable by a surface ship, surface waves and the unstable and non-homogenous nature of the ocean currents. Thus high accuracy motion sensing is mandatory for high resolution SAS.

One possible solution is to use an Inertial Navigation System (INS). However, it is found that even a very high grade INS alone may not provide sufficient accuracy, since the dominant short term position errors of INS are quadratic functions of time [1] and [2].

Data-driven techniques (also termed autofocusing) provide an alternative to instrumentation. A very promising data-driven technique is Displaced Phase Centre Antenna (DPCA) micronavigation. A multi-element receive array is employed to estimate the motion of the sonar by exploring the temporal and spatial correlation of received reverberations from the seabed between adjacent transmissions [3]. Theoretical and experimental studies [4], [5], [6] and [7] have assessed the potential, and the limitations, of this technique. These studies have shown that the achievable SAS performance is limited chiefly by DPCA micronavigation accuracy.

One of the major scientific objectives of the trial was to investigate whether higher navigational accuracy could be obtained by combining DPCA and INS navigation estimates. This would allow more accurate autonomous navigation of underwater vehicles and higher SAS performance. In Section II, we give a detailed description of the experiment and in Section III some preliminary results on the data processing.

II. THE EXPERIMENTAL SETUP

A. The site and equipment

InSAS'00 was carried out in November 2000 in Marciana Marina, Elba Island (Italy). The trial site is illustrated in Fig. 1. It offers an easy access for lab equipment and deployment. The water depth varies between 13 m and 15 m. The wet end equipment was deployed with help of divers and connected to the base lab via cables. It consists of mainly a 20 m rail, a multi-axis motion actuator (MAMA), two sonar receive arrays, 3 sonar transmitters, all provided by QinetiQ and an INS of 0.1 nm grade provided by the NATO SACLANT Undersea Research Centre (Saclantcen).

The height of the rail can be varied from 4 to 7 meters. It was decided to set the height at minimum to allow easy deployment within the harbor since the water depth is only 6 meters at some places near the pier. The rail was assembled on the pier (Fig.2), then lifted by a crane to lower it down into the water. Four solid floats were used to keep the rail afloat just above the water surface. This made the whole structure well above the shallowest water depth within the harbor to avoid any

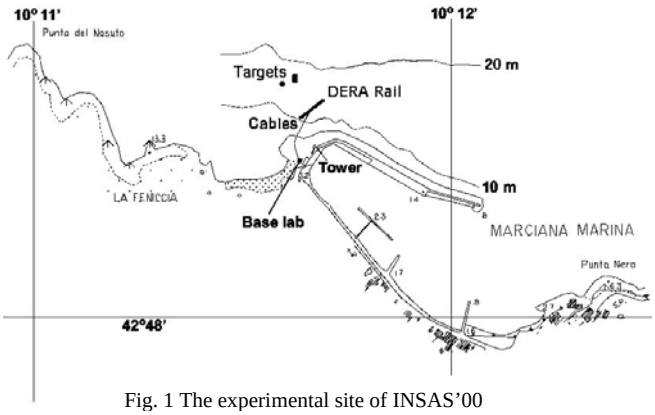

Fig. 1 The experimental site of INSAS'00

Fig. 2 Mobile rail with air bags.

potential structural damage during the towing process from the harbor to the site with a route about 1 km long.

The MAMA can provide variable sway, roll and yaw motions to the sonar with a constant surge. It was used to simulate distortions in the sonar trajectory, similar to those it might be subject to when carried by a towed body or a UUV.

The setup of the sonar and INS on the top of the motion system is shown in Fig. 3. Two 32 element receive arrays of length L=26.7 cm were mounted with 21 cm vertical separation, for interferometric measurements. The beam width of a receiver element is 45° in the horizontal plane and 20° in the vertical plane. There were three transmitter arrays on the top of the receiver housing spaced at L/2. The middle one was aligned with the centre of the receive array. The transmitters are 32 cm high and 2 cm wide. They have a horizontal beam width 28° and a vertical beam width of 2.8°. The INS was rigidly mounted right underneath of the housing of the receive array as a strapdown navigator.

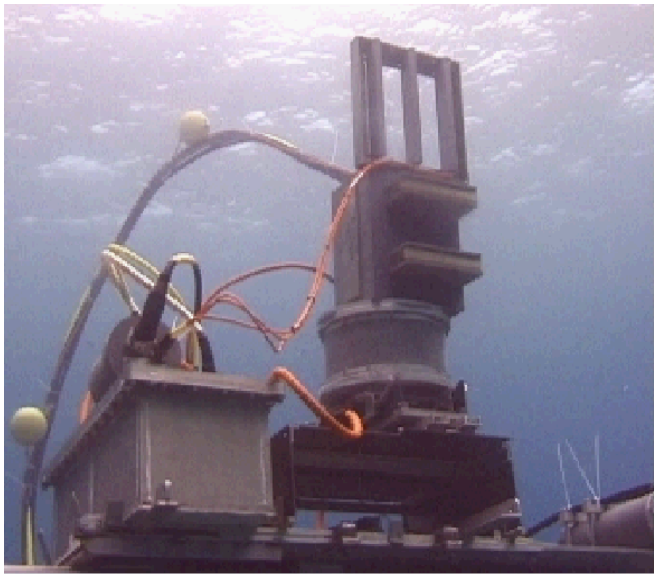

Fig. 3 The sonar and INS on the MAMA system

Throughout most of the trial only a single transmitter was used. The transmitted signal was then a 4 ms linear frequency modulation, swept from 120 kHz to 180 kHz. The transmitters can be driven with simultaneously with different waveforms, which can also be changed from ping to ping. This was used to collect data for the investigation of different modes for SAS with increased area coverage.

There were several different configurations of the target field during the trial. One is shown in Fig. 4. A tripod with one sphere and two bicones is seen at top left about 70 m from the rail. In addition there is a bicycle and a ladder at 55 m, a quarry rock of size of 1.1 m × 0.8 m × 0.8 m, on a turntable at the center. There is also a truncated cone and an extended target of irregular shape at about 50 m. The turntable was operated manually from the shore, with an underwater camera to monitor its rotation. This allows multi-aspect imagery of an object placed on the turntable.

Because of the sloping bottom at the site and the large span of the rail, it was difficult to find a flat area to place the rail horizontally. The rail was deployed on the sea bottom with different depths. One end of the rail is 7.2 m and the other end is 8.5 m below the sea surface measured by divers. This results in a bend of the rail, as seen from the pitch measured in the middle of Fig. 5. The roll of the sonar platform measured by INS during three runs from one end to the other of the rail with a constant speed 6 cm/s indicates the shape of the rail like an "S" in its height shown in the top trace of Fig. 5. There is a 1.5° rotation of the rail around the rail as indicated in the middle trace of Fig. 5. The rail is snaking slightly (0.4°) in the horizontal plane as illustrated at the bottom of Fig. 5. One should notice that the measurements were carried out on two different days. The low frequency variation of the measured data is nearly identical because it is determined by the shape of

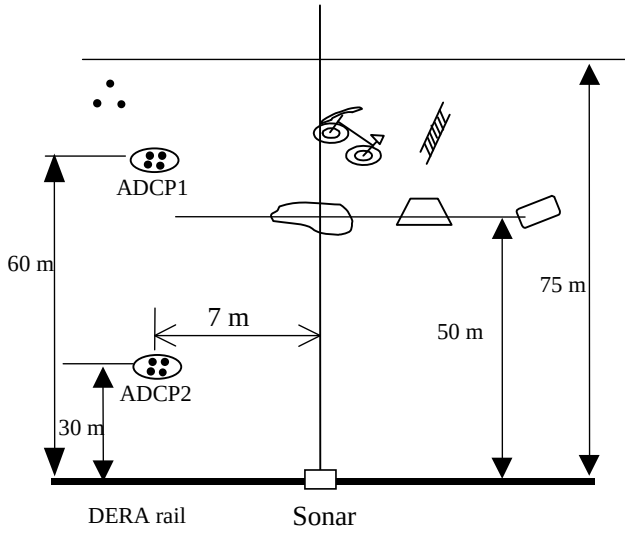

Fig. 4 Target field and sonar

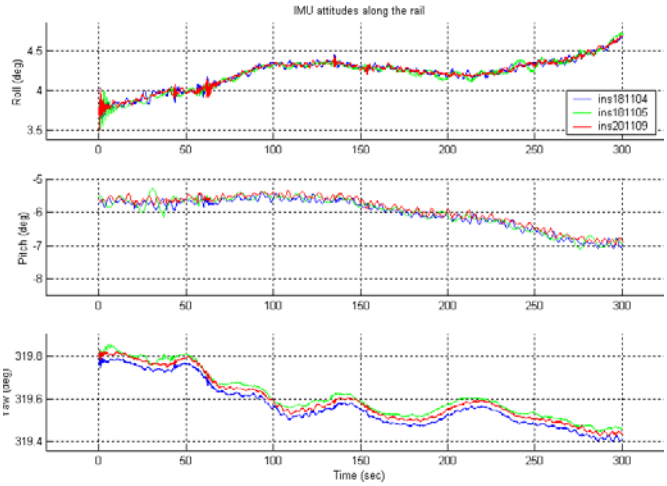

Fig. 5 Roll, pitch and yaw of the sonar moving along the rail

the rail and the speed of the trolley. The high frequency components are due to wave action and jitters as the trolley passed the junction between two sections of the rail. The waves cause random variation, while the jitters are highly correlated as shown in Fig. 6.

Since the rail was made of a number of sections, there were jitters as the trolley passed the joints. These jitters were detected by the accelerometers of the INS as illustrated in Fig. 6. Two identical runs are shown here. The agreement is remarkably good especially for the along track and vertical accelerations. The across track acceleration data indicates that the structure of the MAMA system in this direction is not as stable as in the along track direction. It is susceptible to the external forces such as those induced by waves.

Sidescan survey was carried out at the site. Fig. 7 shows one image from the DF-1000 sidescan sonar working at 400 kHz. The distance between two adjacent red line is 10 m. There were 3 targets at range 40~50 m and 5 targets at range of 70~75 m from the rail in this case. The rail and the sonar on it are clearly visible on the left of the figure. All the targets laid on the sea floor for the trial can also be seen

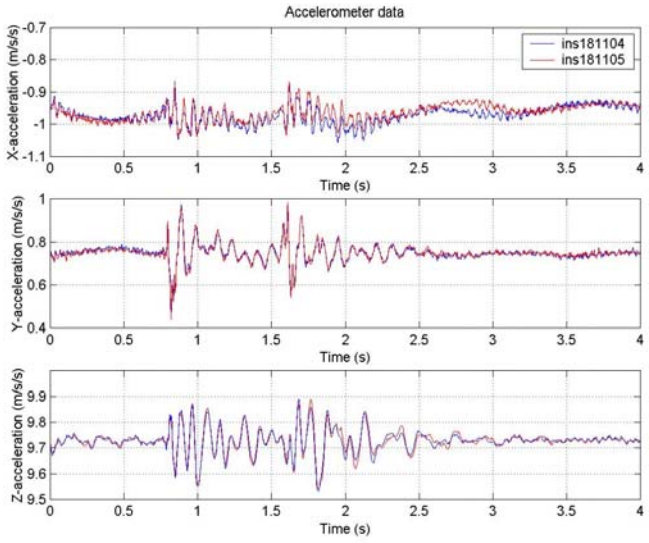

Fig. 6 Raw accelerometer data (prior to gravity correction)

but a mine like object at 75 m is a weak one. There is a large area of outcrop of rocks on the left (seen from the sonar point of view) near the turn table at the distance of 35 m and beyond. A dip on the right side of the turn table is indicated by the low signal return. At long distance from the rail towards the deep water, the slope of the bottom is such that there is very low bottom reverberation. Thus most targets were moved closer to the sonar, at 50 m from the rail, where the slope is not so steep.

B. Environmental conditions

The weather condition changed a lot during the whole period of the trial. Fig. 8 shows measured wave height for the final period of the trail from 18th to 23rd of November. Since the water depth is only 7-8 meter above the rail, the wave activity had strong an effect on the cross track motion of the sonar.

Two ADCPs were deployed to monitor the local current in the field. Sound velocity was also measured *in situ* during the trial. The combination of strong wind and shallow water made the sound velocity almost a constant in the water column. It is expected that sound rays be straight over the distance of interest.

III. PRELIMINARY RESULTS

Only two sonar runs are analyzed in what follows. In both cases the sonar was displaced at a nominal speed of v=6.7 cm/s over a distance of 18 m with a ping repetition rate of 2 Hz, giving a ping-to-ping displacement of D=L/8. The MAMA was used only for the second run to generate a sinusoidal yaw with a period of 7s and 2 degree peak to peak amplitude.

A. Results of DPCA micronavigation.

DPCA micronavigation was performed for both runs with a correlation window of 5 m in range centered at 45 m and 50 m, and the results are plotted in Figs. 10 & 11. A time jitter in the electronic system of signal transmission and reception which corrupted the micronavigation estimates, was found and removed.

The micronavigation estimates the three components of the sonar displacement between successive pings projected in the

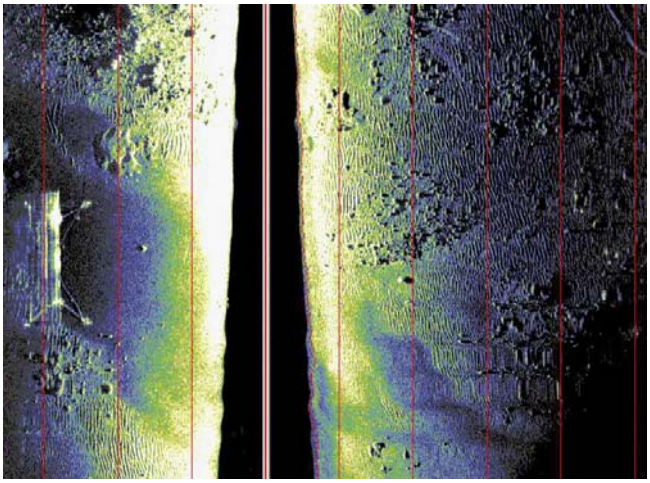

Fig. 7 Sidescan image of the rail and target field

slant range plane, termed DPCA surge, sway and yaw. It should be cautioned that this terminology is slightly misleading since the DPCA surge between two pings (resp. DPCA sway) relates to the linear displacement projected along (resp. perpendicular to) the receive array heading. It is found that the 2 degree peak

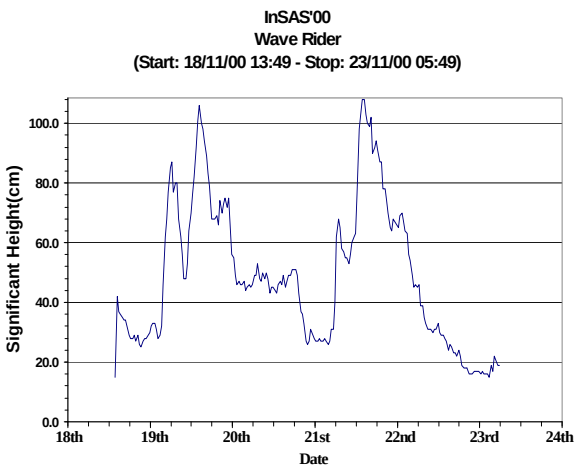

Fig. 8 Measured wave height during the trial.

to peak yaw generated by the MAMA introduces a periodical component in the surge. The effect is also present but less noticeable in the sway because of the lever arm effect.

An average ping to ping correlation of μ=0.9 was found for the chosen correlation windows, giving a theoretical standard deviation ([4]) on the DPCA sway of only 4 μm, and 0.09 degree for the yaw. The number of independent temporal samples is 500 and the number of independent spatial elements in the physical array is 13, giving an effective reverberation to noise ratio of 47 dB (see [4]).

B. INS alignement with Navlab

A brief specification of the INS used in the trial is given in Table I. The raw INS data, *i.e.*, the body acceleration and turn rate measured in inertial space were processed by Navlab, a software developed by FFI, which provides a navigation solution from real or simulated sensor measurements, using the navigation equations and an error state Kalman filter. The block diagram in Fig. 9 describes the main functions of the software.

	Gyro	Accelerometer
Measurement range	±10/10/15°/s	±2g
Resolution	1.13”	0.2 μg
Noise density	0.003° /√h	8 μg/√Hz
Bias	0.003° /h	30 μg
Scale factor	10 ppm	70 ppm
Nonlinearity	10 ppm	15 μg/g^2

Table I. Specification of the INS

In order to perform the initial alignment of the INS, approximately 6 minutes of data were collected with the sonar stationary, immediately before each run on the rail. The alignment was achieved by simulating position and depth measurements, followed by Kalman filtering and smoothing over this period. Values of the position and depth were estimated, using GPS, and white noises of 5 cm standard deviation in both position and depth were added, with a 1Hz update rate, to account for possible sonar motions induced by waves or currents.

It was found that the alignment process was much longer when there were high waves.

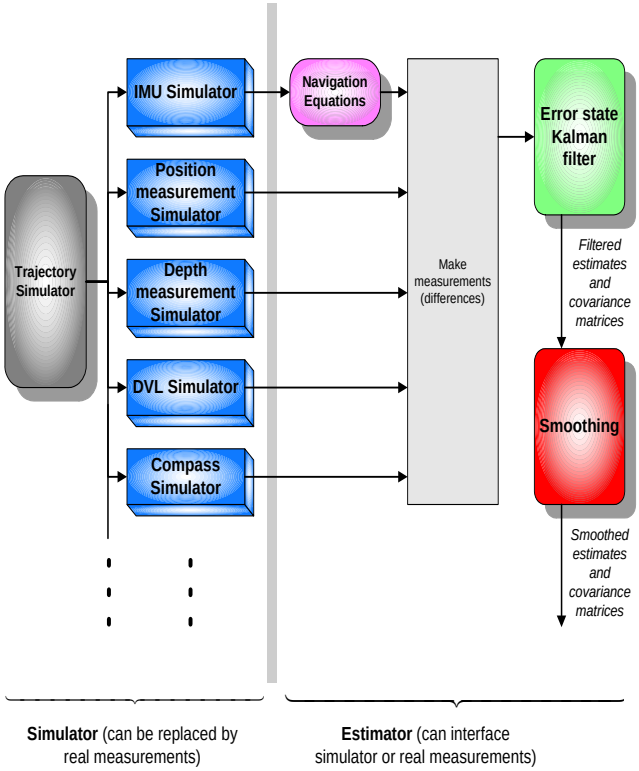

Fig. 9 Block diagram of NavLab

C. Autonomous navigation using DPCA aided INS

Aiding of an INS with external sensors is necessary to reduce the drift inherent in free inertial systems Since the DPCA can provide a very high precision measurement of the ping to ping displacement, it is a good candidate as an external aiding sensor. For reasons of simplicity, the DPCA was treated as an effective DVL. It has to be pointed out that this is an approximation, since the DPCA measures the body velocity in the sonar slant range plane, averaged over the ping repetition period, while DVL measures instantaneous velocity in 3D space. The velocity component normal to the slant range plane is set to zero for the DPCA aiding. The aiding is quite effective as it is demonstrated in Fig. 10. The surge and sway measured by DPCA and aided INS are in good agreement. The standard deviation is 1.3 mm/s for the sway rate and 1.5 mm/s for the surge rate.

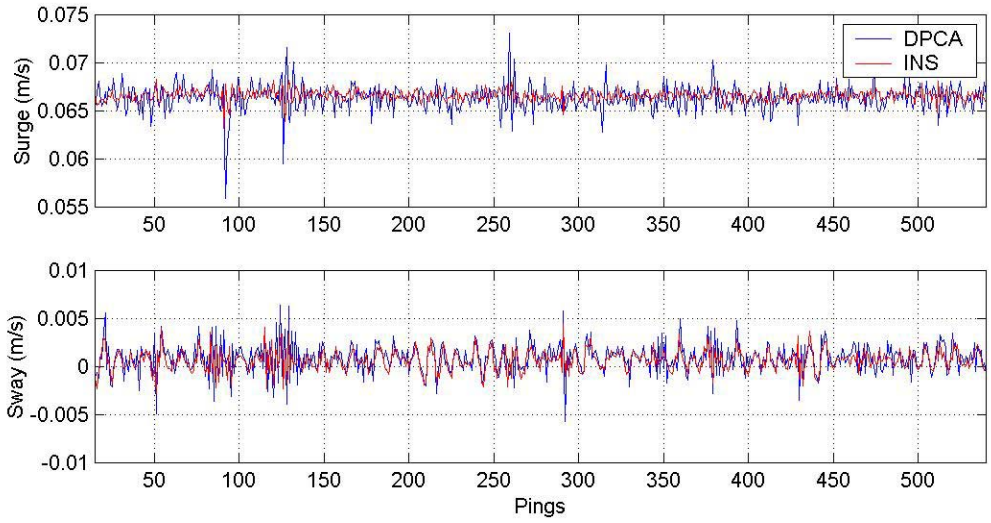

Fig. 10 DPCA and DPCA-aided INS velocities (no yaw).

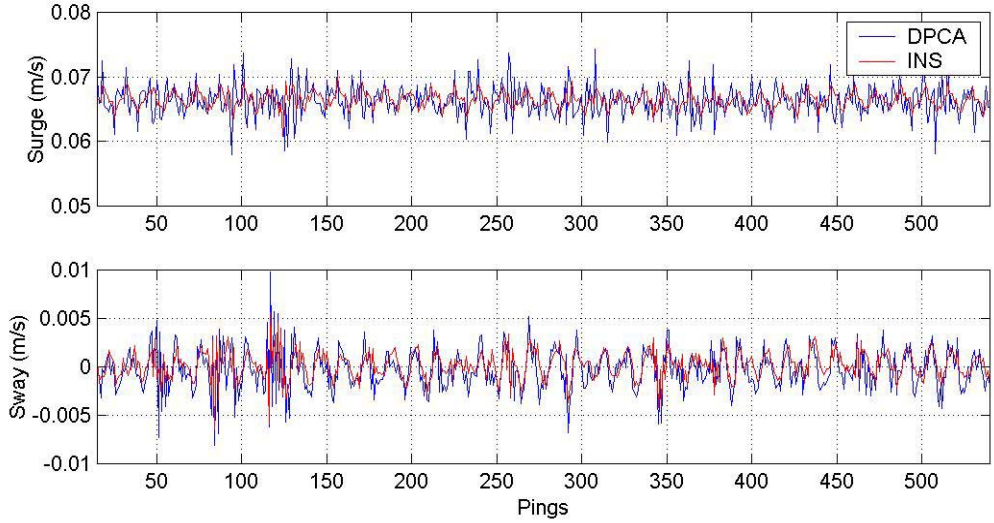

Fig. 11 DPCA and DPCA-aided INS velocities ($\pm 1^{o}$ MAMA yaw).

The aided INS result with the simulated 2 degree yaw is shown in Fig. 11. The difference between the INS and DPCA results is greater compared with the previous case in Fig. 10 due to the large yaw introduced. The standard deviation is 1.4 mm/s for the sway rate and 2.5 mm/s for the surge rate. This should compare favorably with traditional aiding with a DVL.

D. Free inertial navigation during SAS integration time

An alternative method to combine the INS and the DPCA is to perform free inertial navigation solution during an SAS run, after the stationary alignment, and use the DPCA to remove the drifts due to alignment errors. All the geometric corrections required to make the INS solution directly comparable to that of DPCA were performed. These include the lever arms between the centre of the INS and that of the transmitter and that that of the receive array, and slant range projection. The results are plotted in Figs. 12 and 13 together with the DPCA results.

The drifts have been removed in Figs 12 & 13 by fitting, by least squares, a third order polynomial to the difference between the INS and DPCA surge and sway estimates. The standard deviation of the difference of the results between the INS and DPCA in Fig. 12 is 0.1 mm for both the surge and sway (0.2 mm/s for the surge and sway rates). In Fig. 13 this standard deviation increases up to 0.15 mm for the surge, 0.16 mm for the sway (0.3 mm/s and 0.32 mm/s for the corresponding rates). This increase in the standard deviation compared with the previous run is believed to be due mainly to the uncertainty in the measurement of the lever arms, which introduce larger errors in presence of bigger sonar motions.

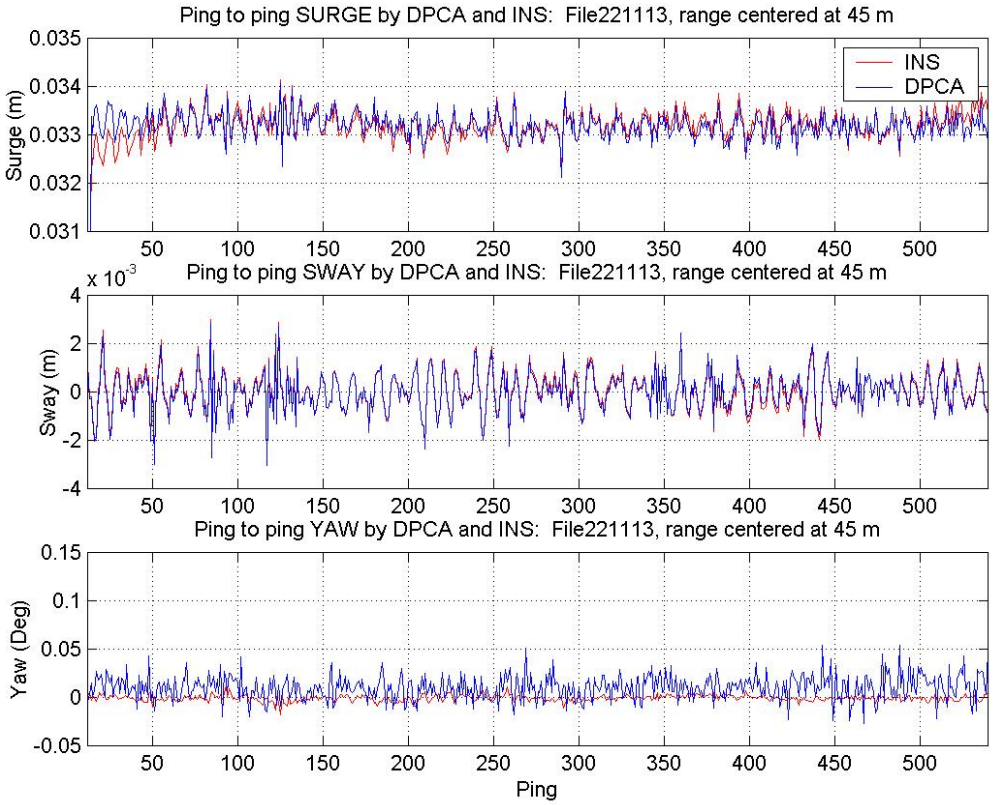

Fig. 12 Ping to ping surge, sway and yaw of the sonar measured by DPCA and INS with no simulated yaw.

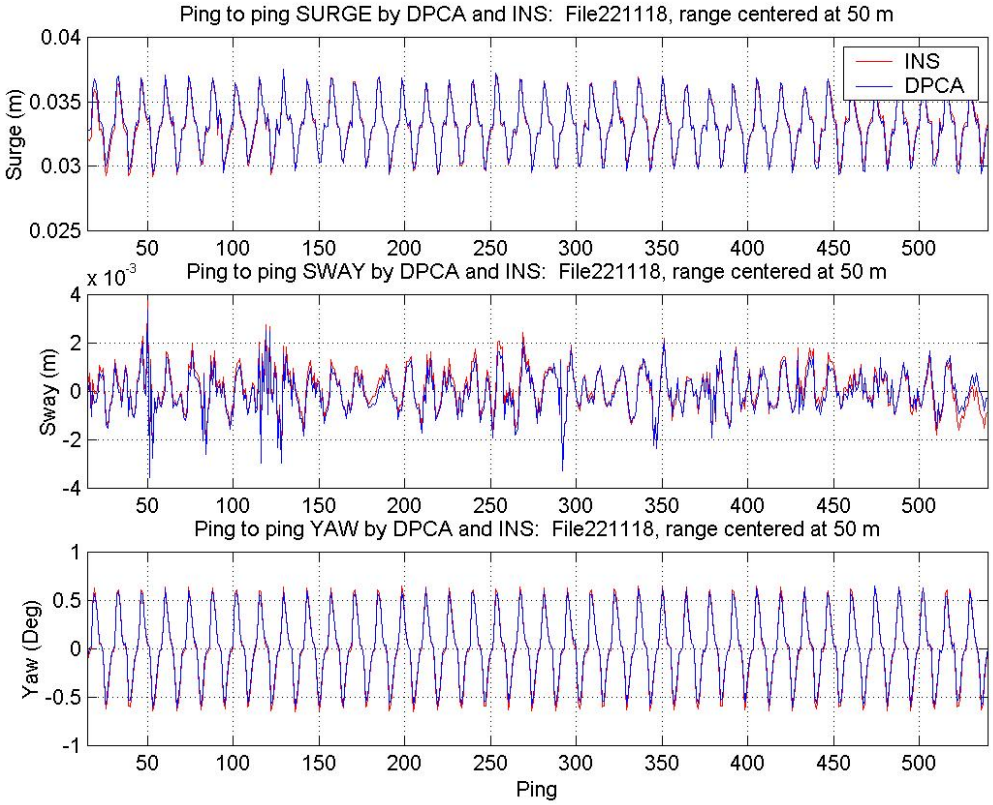

Fig. 13 Ping to ping surge, sway and yaw of the sonar measured by DPCA and INS with ±1° MAMA yaw.

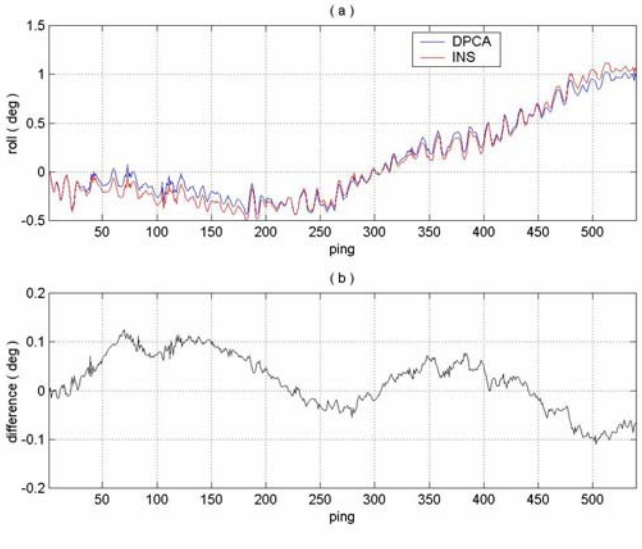

Fig. 14 Sonar roll measured by DPCA and INS

However, there is a significant difference between the INS and DPCA yaw estimates, as shown in the third part of Figs. 12 & 13. In Fig. 12 (resp. Fig. 13) the standard deviation of the difference of the two measurements is 0.014 degrees (resp. 0.031 degrees). This is expected since the theoretical accuracy of the DPCA yaw, is significantly worse than that of the INS which is in the range of 5×10^{-5} degrees (based on the specified white noise of the ring laser gyros). In addition the DPCA yaw estimate is seen to be biased and in Fig. 13 a scale factor is also apparent.

E. Roll measurement with interferometric sonar

An accurate measurement of the roll is important when measuring bathymetry with interferometric sonar. One way to measure the roll is to use the DPCA micronavigation results for both the top and bottom arrays ([8]). Fig. 14(a) shows a comparison of the INS roll (red curve), with that obtained using the DPCA micronavigation estimates for both arrays of the sonar (blue curve). The roll estimates are relative to the first ping in order to facilitate the comparison with the DPCA algorithm that works on a ping-to-ping basis. The DPCA roll is given by the difference in sways of the two arrays, divided by the separation of their corresponding phase centres. Prior to estimating the difference in sways, any misalignment of the two banks has to be corrected since this will introduce an spurious linear roll. This linear roll is estimated from the angle of rotation between the SAS images that maximizes the cross-correlation of the images (see [8]). Fig. 14(b) shows the difference between the INS and DPCA roll estimates. Some minor systematic discrepancies remain which require further clarification.

F. SAS imaging

Figure 15 (top) shows the conventional sonar image of the target field using a single ping at about 8 m from the left side of the rail. There are four targets in this image. They are the truncated cone at (7 m, 49 m), a mine like object at (10 m, 50 m), a bicycle at (8 m, 57 m) and a ladder at (12 m, 56 m). One should notice that the bicycle is a very strong target due to the air inflated tyres, while the rungs of the ladder are visible, but it is impossible to identify them in this image. The bicycle and ladder can not be clearly identified as two separate targets due to the low along track resolution. The shadow strip on the top of the figure is the result of truncation of received signal in time domain in order to reduce the time to process and storage space.

Fig. 15 (middle) shows a SAS image of the same target field for the run with MAMA yaw. The increase of the along track resolution makes possible to separate the bicycle and ladder. 8 rungs of the ladder can be counted unambiguously from this image. Some shadows are formed behind the targets at the bottom of the image. However, the shadows are partly filled with scattered signals from the relative rough bottom.

Two hundred pings were used for the image which corresponds, for a ping to ping displacement D = L/8 (α=L/2D=4), to a theoretical along-track resolution gain Q=50 (Q is the ratio of the resolution of the physical array to that of the synthetic array). The 3 dB along-track resolution of the SAS image was measured close to 4 cm, prior to shading with a Hanning window and is indeed Q=50 times smaller than that of the physical array of 26.7 cm. The micronavigation data from Fig. 13 was used, combining the DPCA sway and surge estimates with that of the INS yaw.

Operation at α=4 is a limitation from an practical point of view since it increases the length of the physical array required to operate at a given platform velocity and maximum range. For example, operation up to 200 m range at 3 knots would require a physical aperture of 3.2 m which is very long indeed.

To assess whether this limitation could be relaxed, the micronavigation and the SAS imaging were repeated, for the same run, with only one half of the physical array, i.e. the 16 central elements instead to the total 32 elements, reducing the spatial oversampling factor from α=4 to α=2. The micronavigation accuracy of the DPCA is expected to degrade with the halving of the number of elements in the DPCA. However the SAS image, shown in Fig. 15 (bottom), is very similar to that in Fig. 15 (middle). Its 3 dB along-track resolution is again close to 4 cm, that is Q=100 times smaller than that of the physical array, now of length 13.35 cm.

The estimated SAS trajectories for α=4 and α=2 are compared in Fig. 16 (top). These trajectories are in the slant range plane with x_p along-track and y_p across-track. The differences in across-track position Δy_p (resp. along-track position Δx_p) between α=4 and α=2 are plotted in the middle (resp. bottom) of Fig. 16. In both cases these are obtained by combining the DPCA sway and surge estimates with that of the INS yaw. The SAS was formed between pings 286 and 486.

To see the improvement of micronavigation accuracy brought by the INS, the above SAS trajectory for α=2 is compared with the trajectory obtained with the DPCA yaw estimate in the Fig. 17 (top). The difference in across-track position Δy_p (resp. along-track position Δx_p) between both cases is also plotted in the middle (resp. bottom) of Fig. 17. Due to large errors in yaw, the DPCA solution is seen to drift. In this plot a parabolic drift was removed, by curve fitting, to the Δy_p

to account for the bias in the DPCA yaw noted in Fig. 12. Since the effective reverberation to noise ratio is now 44 dB, it follows from [4] that the highest achievable Q by DPCA micronavigation is of the order of 15, i.e. a maximum of P=30 pings since α=2. This is about 100/15=6.7 times less than when both the DPCA and the INS are used together.

IV. SUMMARIES

The InSAS'00 trial has provided us a large amount of data for analysing the performance of SAS under well controlled and accurately measured motion conditions. Preliminary analysis has shown that the combination of DPCA and INS allows higher navigational accuracy and therefore higher performance SAS imagery.

ACKNOWLEDGEMENTS

The trial is a part of Joint Research Project led by Saclantcen in which QinetiQ and FFI are active partners. The authors would like to thank all the people involved in this trial, especially, engineering coordinator, L. Troiano, T-boat captain A. Iacono and L. Gualdesi, M. Mazzi and M. De Grandi, for their indispensable contributions.

REFERENCES

[1] "Synthetic aperture sonar motion compensation system. Analysis and simulation study," Tech. Rep. 40910020-R0, Applanix (Applied Analytics Corporation) and TSS, March 1997.

[2]. A Tesei and M. Pinto, "Application of aided inertial navigation system to synthetic aperture sonar micronavigation," Saclantcen Memorandum SM-368, 2001.

[3]. M. Pinto, F. Fohanno, O. Tremois and S. Guyonic, "Autofocusing a synthetic aperture sonar using the temporal and spatial coherence of seafloor reverberation," in *High frequency acoustics in shallow water*, edited by N. G. Pace et al, pp 417-424, 1997.

[4] A. Bellettini and M. Pinto, "Theoretical accuracy of synthetic aperture sonar micronavigation using a displaced phase centre antenna," submitted to *IEEE J. Ocean. Eng.*, 2000.

[5] G. S. Sammelmann, et al, "High frequency/low frequency synthetic aperture sonar," *Naval research reviews*, Vol. 49, pp. 3-8, 1997.

[6] D. Billon and F. Fohanno, "Theoretical performance and experimental results for synthetic aperture sonar self-calibration," Proc. Oceans'98, pp. 965-970, Nice, 1998.

[7] M. Pinto, A. Bellettini, S. Fioravanti, S Chapman, D. R. Bugler, Y. Perrot and A. Hetet, "Experimental investigation into high resolution sonar systems," Proc. Oceans'99 Seattle, 1999.

[8] M. Pinto, R.D. Hollett, A. Bellettini, S. Chapman, "Bathymetric imaging with wideband interferometric synthetic aperture sonar", submitted to *IEEE J. Ocean. Eng.*, July 2001.

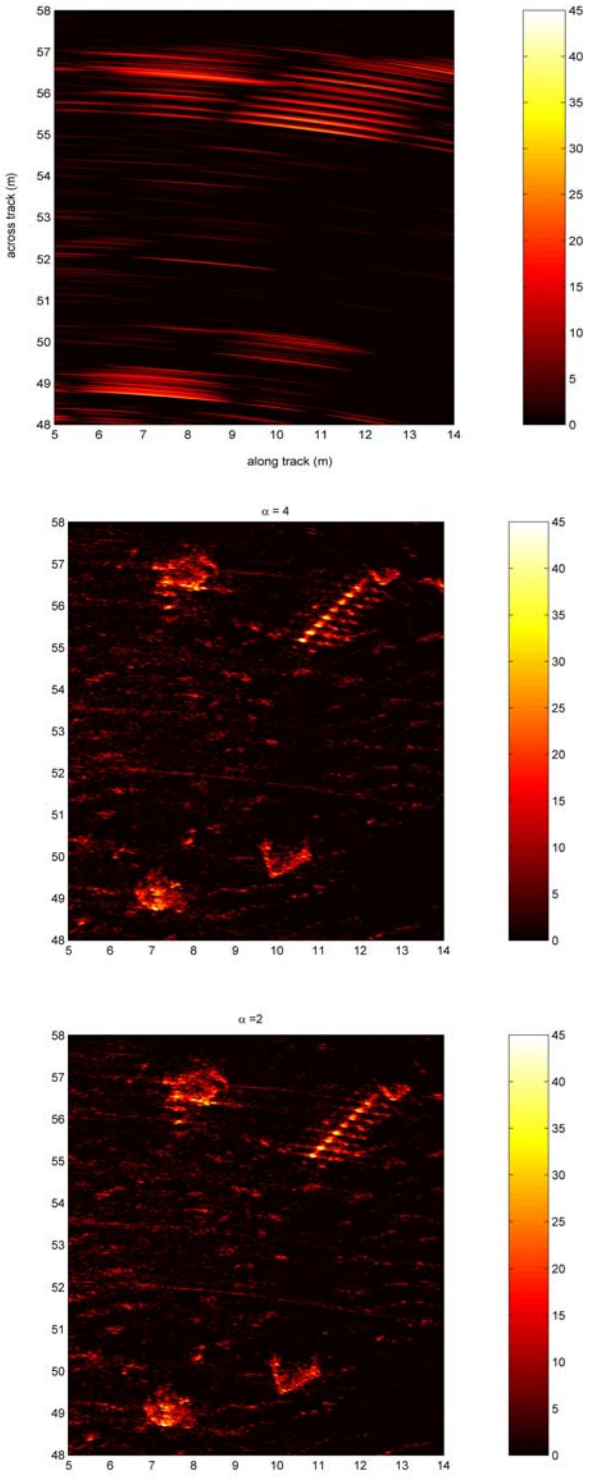

Fig. 15 Physical image (top) and SAS images (middle and bottom) for $\pm 1^{o}$ MAMA yaw and DPCA+INS micronavigation. The bottom SAS image is obtained with only the central half of the physical array.

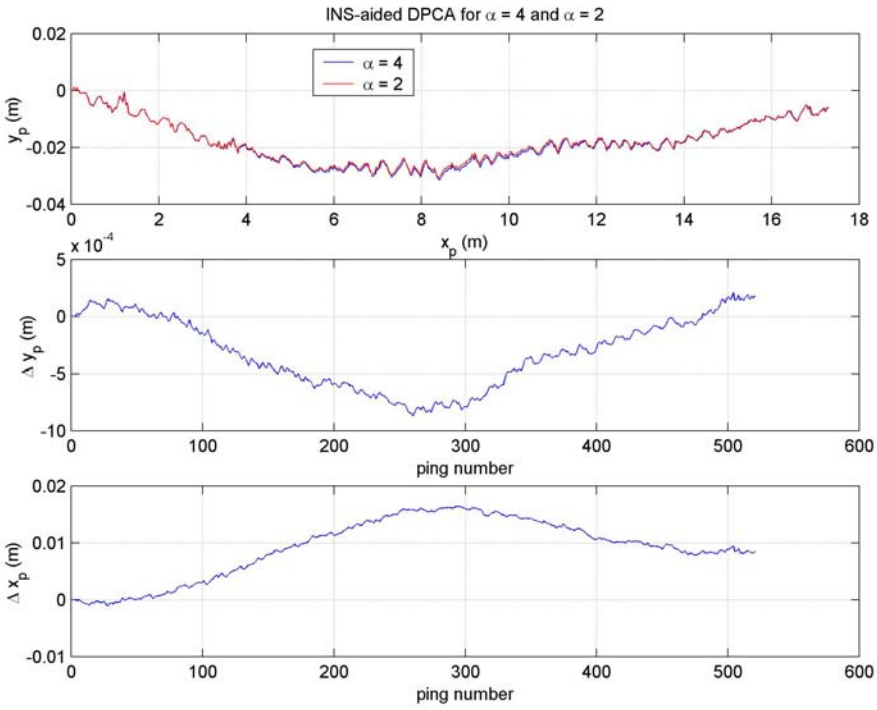

Fig. 16 SAS trajectory estimates obtained using DPCA+INS micronavigation with the full physical array (α=4) and only the central half (α=2). The across-track and along-track differences Δy_p and Δx_p between both trajectories are plotted in the middle and bottom graphs as a function of ping number.

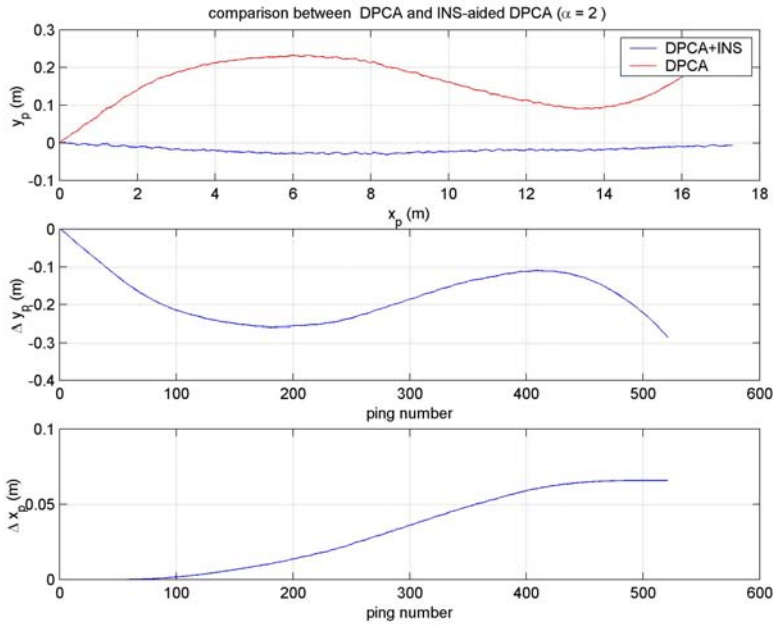

Fig. 17 SAS trajectory estimates obtained using DPCA+INS micronavigation (blue) and DPCA micronavigation (red) for (α=2). The across-track and along-track differences Δy_p and Δx_p between both trajectories are plotted in the middle and bottom graphs as a function of ping number.